Journal of Applied Polymer Science

Adjustable amine–epoxy composition in a stratified thin film with a spin-coating process: A useful tool for establishing relationships between the local glass-transition temperature at the interface and the network structure

Pascal Carriere, Sandra Onard, Isabelle Martin, Jean-François Chailan
Laboratoire Matériaux, Polymères, Interfaces et Environnement Marin (EA 4323), Université de Toulon, Avenue de l'Université 83957, La Garde Cedex, France
Correspondence to: P. Carriere (E-mail: pascal.carriere@univ-tln.fr)

ABSTRACT: An easy method for preparing supported homogeneous epoxy–amine thin films on a silica surface consisting of two distinct layers was developed via spin coating from epoxy–amine solutions. Because of these two layers had the controlled properties of the upper layer, we showed that it was possible to precisely control the epoxy–amine stoichiometry in the sublayer through the initial epoxy–amine ratio, the spin-cast process, and the overall film thickness. First, in the thin films, the primary amine–epoxy conversion was constant, whatever the thickness and initial epoxy–amine stoichiometry for a given curing schedule. As the primary amine conversion can be independently tuned in thin films, it thus provided a rather unique and easy method for better understanding the relationship between the network structure curing at the interface and the resulting properties, such as the glass-transition temperature (T_g) and elastic modulus. Here, we also showed that we could access the local T_g; this implied a potential application of these experimental data in predictive composite material properties. © 2015 Wiley Periodicals, Inc. J. Appl. Polym. Sci. **2015**, *132*, 42078.

KEYWORDS: coatings; crosslinking; glass transition; properties and characterization; thermosets

Received 20 September 2014; accepted 4 February 2015
DOI: 10.1002/app.42078

INTRODUCTION

Epoxy networks, built up from diepoxides and diamines, are materials that are widely used in industrial applications; these include adhesives, coatings, electronics encapsulation, and high-voltage isolation, as well as fiber- and particulate-filled epoxy composites and matrices for composite materials.[1–3] They are selected for their high performances (lightness and mechanical and thermal properties) achieved through synthesis and processing. Numerous studies have been devoted to the dependence of the viscoelastic properties, solvent–water ingress or fracture behavior on the chemical structure at the molecular level. Some of these studies have essentially dealt with commercial products whose structures are not well defined or have only considered the main epoxy–amine reactions.[4–8] That is why prior results are somewhat conflicting or make fundamental insight difficult to extract from complex formulations. Nevertheless, fundamental studies have been conducted in parallel to fill this gap with well-defined[9–13] or systematically varying network structures,[14,15] including epoxy–amine water-uptake mechanisms.[16,17]

With regard to epoxy–amine systems, it has been shown that in addition to the classical addition of amine functions to epoxide groups, other reactions involving the addition of secondary alcohol functions to the epoxide functions or the homopolymerization of epoxide functions may occur. The solution of the problem appears important in practice because the curing of epoxy resins with amine hardeners is often performed for practical purposes in the presence of catalysts that promote these side reactions or in the presence of excess amine to toughen the matrix.[18] Otherwise, with regard to epoxy–amine resins directly cured in the presence of a solid surface, several workers have suggested that the stoichiometry and the curing process are also affected at the solid surface.[19] Several authors have explored the sensitivity of composite material properties, including the thermoelastic behavior, which is affected by variations in the epoxy–amine stoichiometry at the interfaces. They showed that the modulus and glass-transition temperature (T_g), among others, were significantly affected by these variations in the stoichiometry.[20,21] Thus, the crosslinking density varied as a function of the diamine–epoxy ratio and the curing conditions.[22]

Additional Supporting Information may be found in the online version of this article.

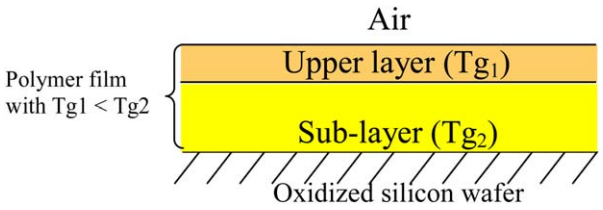

Figure 1. Schematic representation of stratification in the epoxy–amine films (the amine–epoxy ratio in the whole film was equal to 1.13 before curing).[17] [Color figure can be viewed in the online issue, which is available at wileyonlinelibrary.com.]

Yim *et al.*[23] reported that the composition modification of 80-nm thin films was limited to a few angstroms at the polymer–substrate interface, whereas a great enrichment of the crosslinker at the air–polymer interface was noticed. These segregation phenomena strongly affected the polymer network structure in the film by creating two distinguishable layers (Figure 1) with different crosslinking densities. Recently, we highlighted that this preferential segregation in thermoset-supported films with a whole amine–epoxy ratio of 1.13 before curing and thicknesses in the range 100–300 nm was at the origin of the two T_g's.[24,25] We also showed that the network structure and properties of the sublayer of thin diglycidyl ether of bisphenol A (DGEBA)–diphenyl diaminomethane (DDM) films were affected by the epoxy–amine stoichiometric imbalance induced by phase segregation,[25] along with increasing etherification with excess epoxy.

The purpose of this study was to use this original property of vertical stratification in thin DGEBA–DDM films to perform a systematic study on the initial stoichiometry effect on the network structure curing at the interface in excess amine and to reduce the gap between the identification of the network structure at the interface at the molecular level and the corresponding local T_g.

Otherwise, T_g was assumed to be thickness-dependent below 90 nm. Wang and Zhou[26] studied the T_g of a microtome-sliced epoxy thin film from a fully cured bulk sample. A T_g depression of 15 K was observed for a 40-nm thin film as compared with the bulk sample. These results were confirmed by the molecular dynamics in ultrathin freestanding thermoset films.[27,28] Likewise, Lenhart and Wu[29] showed that deviation on the expansion coefficients at the rubbery state from bulk to confined thermoset films occurred in the range of 20–40 nm film thicknesses for thin thermosetting films supported on a silicon surface. This deviation was observed, whatever the surface treatment used for modifying the surface energy and polymer–surface interactions. To prevent a confinement effect on the relationships between the network structure at the air–film interface and T_g, the film thickness was kept between 90 and 200 nm.

To achieve this aim, we thus performed on these supported thin films microthermal analysis used as thermomechanical analysis, which yielded the local T_g. We first describe the film nanostructuration, crosslinking reactions, network structure, and corresponding T_g's of the thin films prepared in excess amine [the ratio of amine functions to epoxide functions $(r) = 1.4$]. The sample in excess amine was postcured, and we demonstrate that the epoxy groups were fully consumed. Then, through the variation in the film thickness, we show that the confinement effects were not sensitive in the range 100–300 nm. Therefore, we finely controlled the amine conversion rate in the thin films at different epoxy–amine stoichiometries by comparison with the bulk sample, and we discuss the establishment of relationships between the local T_g's at the interfaces and the network structure.

EXPERIMENTAL

Materials

The epoxy resin, based on DGEBA, was purchased from Hempel with a molar mass of 385 g/mol ($n = 0.16$) and was cured with DDM purchased from Sigma-Aldrich (99.9%).

Silicon wafers (100) were purchased from Mat Technology. They were immersed in a piranha solution for 30 min at 70°C, rinsed with deionized water, and dried under a flow of argon before use.

The thermal curing of the thin films was carried out with a VWR model 400 temperature-controlled hot plate in air.

Sample Preparation

The thin, supported polymer films used in this study were obtained by the spin-coating of a toluene solution of a DGEBA–DDM mixture on oxidized silicon wafers at an accelerate rate of 2500 rpm/s and a spin speed of 3000 rpm for 30 s.

The solution mixtures were characterized by $r = [NH]/[EP]$. This means that the stoichiometric mixture of the two DGEBA molecules to one diamine molecule corresponded to $r = 1$. In this study, various ratios were chosen for the solutions ($rs = 1.13$ and 1.4) to prepare quasi-stoichiometric films and amine-rich films. Then, the samples were degassed *in vacuo* at room temperature for 15 min and cured under atmospheric pressure according to the following schedule (stage 1): 1 h at room temperature, 1 h at 50°C, 45 min at 75°C, and 30 min at 110°C. First, the concentration of the epoxy solution was fixed at 55 g/L to obtain homogeneous thin films about 200 nm thick. A detailed discussion of the sample preparation is given elsewhere.[24] Then, microthermal and IR characterizations were performed. An additional postcuring of 2 h at 180°C under argon was also applied to the samples after the first characterizations to complete epoxide conversion.

To study the influence of the film thickness on the sample properties after curing according to stage 1, the concentration of the epoxy solution was varied from 25 to 80 g/L.

Instrumentation

Microthermal Analysis. Local T_g measurements were carried out on a TA Instruments 2990 microthermal analyzer. Probe temperature calibration was performed at room temperature and with the differential scanning calorimetry peak melting point of poly(ethylene terephthalate). With the microthermal analyzer localized thermal analysis (L-TA) mode, the probe was held in place at a location selected on the surface with a force of 12 nA; this corresponded to 20–30 μN, and its temperature was usually raised from 25 to 250°C at 15°C/s and then cooled to 25°C. The vertical position of the probe during heating was

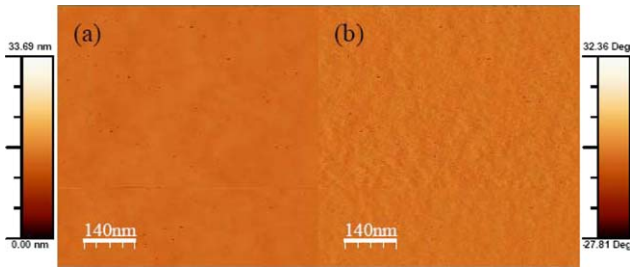

Figure 2. Tapping-mode AFM images of epoxy–amine films cured on oxidized wafers: (a) height image and (b) phase image for amine-rich films ($r = 1.4$). [Color figure can be viewed in the online issue, which is available at wileyonlinelibrary.com.]

followed by laser displacements focus on the probe (localized thermomechanical analysis or sensor signal).[30,31] The probe was then moved of 10 μm between each L-TA measurement to make sure that each microthermal analysis was not perturbed by the previous ones.

Infrared Reflection Absorption Spectroscopy (IRRAS). IRRAS spectra were obtained with a Fourier transform infrared spectrometer Thermo-Nicolet Nexus (FT-IRRAS). All spectra were recorded at an incidence angle of 50° to analyze the whole thickness of the polymer films.[32,33] A BaF_2 wire grid polarizer (Specac) was used to select the *p*-polarized radiation. The efficiency of the polarizer was specified to be better than 99% for wave numbers lower than 3300 cm^{-1}. A second ZnSe lens (38.1-mm focal length) was used to focus the reflected beam onto a photovoltaic Mercury Cadmium Telluride (MCT) detector cooled at 77 K. The MCT detector was set onto X, Y, and Z microcontroller stages to optimize the intensity of the focused IR beam.

Six hundred scans were recorded at a resolution of 4 cm^{-1}. A cleaned silicon wafer was used for the reference spectrum. FT–IRRAS spectra allow us to check that the whole epoxy–amine ratio of all of the films before curing corresponded to the initial epoxy–amine ratio in solution. The spin-coating process did not preferentially remove one of the reactive components. FT–IRRAS was also used to determine the epoxide and primary amine consumptions after curing and postcuring. Note that the conversion amine or epoxide rate was calculated from the initial amine or epoxide concentration and the final concentration at the curing schedule achievement. The conversion rates presented hereafter were not normalized by the initial excess amine.

Atomic Force Microscopy (AFM). AFM measurements were performed in tapping mode with a Nanoscope II A instrument (Digital Instruments) with commercially available silicon microcantilever probe tips. Topographic and phase images (0.7 × 0.7 μm^2) were obtained simultaneously with the resonance frequency of the probe at about 270 kHz. The *z* signal was calibrated by steps on a grid with controlled 1-nm steps. The system sensitivity was determined from force measurements on a rigid sample.

X-ray Photoelectron Spectroscopy (XPS) Analysis. The XPS analyses were recorded on a Scienta 200 electron spectrometer equipped with an Al monochromatic source (Al Kα energy = 1486.6 eV). High-resolution spectra were recorded at a power of 225 W for the thin DGEBA films. The electron emission angle was 0° for an analysis depth of lower than 10 nm. We obtained the spectra by setting the instrument to the slot mode and providing an approximately 300 × 700 μm^2 analysis area. The binding energy scale was corrected for static charging with a binding energy of 285.0 eV for the C1s level of aliphatic hydrocarbon. The spectra were tested with the help of the Vision processing fit program. In curve fitting, the full widths at half maximum for all of component peaks were constrained to be equal. Quantification and peak fitting of C1s and N1s, on the basis of the high-resolution spectra, were obtained with this software.

RESULTS AND DISCUSSION

Stratification over the Gradient Properties of the Epoxy–Amine Network

Spin-Coating-Process-Induced Controlled Structure of the Thin Epoxy–Amine Films. Studies concerning the morphology of cured epoxy resin systems have generated many controversies in the literature. Indeed, some studies have suggested the existence of high-crosslinking-density nodules in a matrix of relatively low crosslinking density,[34] whereas others have revealed a homogeneous structure at the nanometric scale.[35] Similarly, epoxy–amine ultrathin films crosslinked at the surface (< 50 nm) were shown to be nanostructured films by the nodules described previously as induced by the epoxy molar mass, nonstoichiometric epoxy–amine ratio, and different surface wetting behaviors between the amine and epoxy[36] or by enrichment of one of the components at interfaces, which led to a crosslinking gradient in the film.[31]

Recently, we showed that thin DGEBA–DDM films cured with an amino hydrogen to epoxide ratio ($r = [NH]/[EP]$) equal to 1.13 lead to a homogeneous lateral surface network on a submicrometer scale and associated with a vertical stratification of the network characterized by two T_g values (T_g's = 98 and 142°C).[25]

To definitely prove that stratification characterized the network morphology of our films, thin films were prepared from spin-cast epoxy–amine solutions at a reduced acceleration rate of 1000 rpm/s. Solvent evaporation coupled the liquid-phase diffusive transport of the solvent toward the interface to the gas-phase convective mass transport of the solvent away from the interface. The solvent vapor was carried away in a stream of air that was drawn down axially toward the surface and driven radially across it by a centrifugal pumping action created by the spinning substrate. As a result, a reduction of the acceleration rate induced a decrease in the evaporation rate, and the migration of the more volatile components (amine or epoxy) was less driven at the air–film interface. Therefore, constituents that needed to further interdiffuse for the crosslinking reaction during curing were probably more homogeneously spread into the films, and this resulted in more homogeneous crosslinking networks.

A film based on a toluene solution of the DGEBA–DDM mixture at 45 g/L ($r = 1.13$) was prepared at 1000 rpm/s to reach roughly a 200 nm thick film. This film was cured with the same

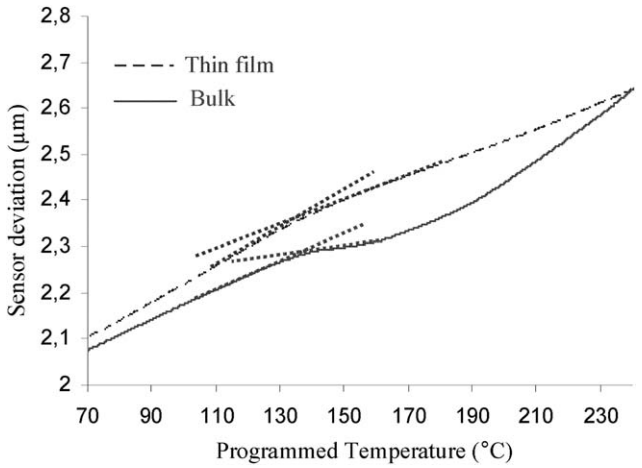

Figure 3. Sensor height position response versus temperature for the epoxy–amine films ($r = 1.13$) prepared at a reduced acceleration rate (1000 rpm/s) and cured according to stage 1 on the same sample (i.e., without postcuring at 180°C).

curing schedule as the films prepared at 2500 rpm/s. The surface morphology of both cured thin polymer films showed a homogeneous surface by AFM with a roughness of about 0.5 nm, as illustrated, that is, for the amine-rich films [Figure 2(a)]. We also noted that the phase imaging contrast did not show any differences in the viscoelasticity response of the surface [Figure 2(b)]. Therefore, we concluded that the roughness was negligible and did not affect the L-TA measurements.

Unlike those of the thin films prepared at 2500 rpm/s, which exhibited two T_g values (98 ± 5 and 142 ± 6°C),[25] the L-TA measurements made on the thin, supported epoxy–diamine films prepared at 1000 rpm/s showed only one broad T_g (131 ± 6°C) with the assumption of a crosslinking gradient into this film (Figure 3). The T_g measured previously for the film prepared at 1000 rpm/s could only be understood as an average property of a film with a crosslinking gradient density. Indeed, the equivalent bulk T_g measured by L-TA ($135°C \pm 7°C$) was

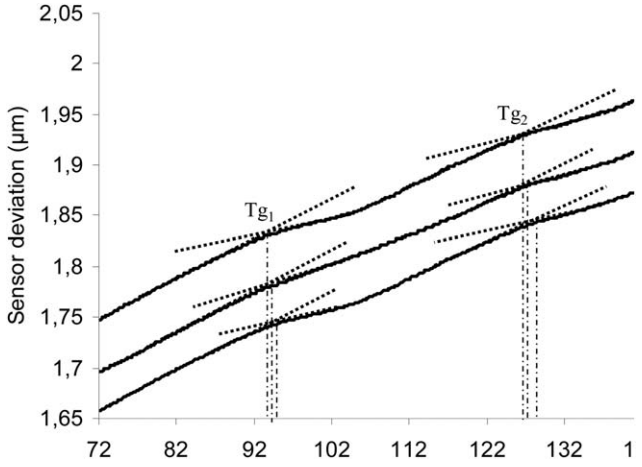

Figure 4. Sensor height position response versus temperature for the amine-rich films ($r = 1.4$) cured according to stage 1 on the same sample (i.e., without postcuring at 180°C).

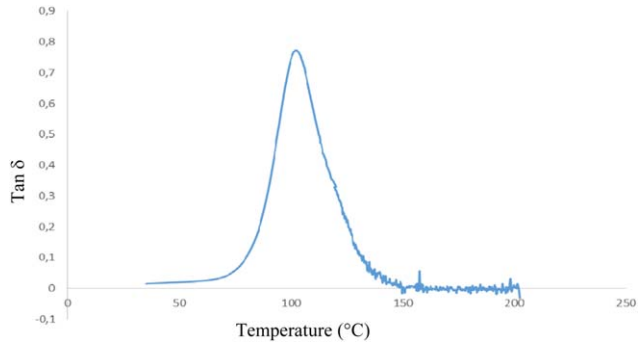

Figure 5. Evolution of tan δ versus temperature for a DGEBA–DDM ($r = 1.4$) bulk sample cured according to stage 1. [Color figure can be viewed in the online issue, which is available at wileyonlinelibrary.com.]

narrower and close to that of one of the thin films. Therefore, there was no evidence that T_g in the surface was lower and could be counted as the reason for the T_g depression of the overall thin film observed for thicknesses above 90 nm.[28] However, in thermoset films, there is also another contributing factor to T_g depression: a change in the conversion degree. Tacking these factors into account, the two distinguishable T_g's observed in the amine-cured epoxy thin films prepared at 2,500 rpm/s, may not have been due to a slight surface T_g reduction but mainly to differences in the crosslinking density; this is discussed in the next part.

Stratification Existence in Off-Stoichiometry Thin Epoxy–Amine Films. The results of some L-TA measurements made on thin, supported epoxy–diamine films with an off-stoichiometry composition ($r = 1.4$) of about 200 nm thick, spun cast at 2500 rpm/s, and cured according to stage 1 are shown in Figure 4. The sensor signal showed two T_g's on every analyzed polymer film. However, in the literature, changes in resin microstructures have been observed as a function of the epoxy–amine stoichiometry[30,33] and sometimes show multiple T_g's. Off-stoichiometry bulk samples ($r = 1.4$) at the same amine conversion rate as thin films revealed only one relaxation by dynamic mechanical analysis (Figure 5). Thus, we could assume that the off-stoichiometry epoxy–diamine thin films were also vertically stratified.

Properties of Layers Structuring Epoxy–Amine Films of About 200 nm

The existence of two T_g's for the whole films and the homogeneity of the network surfaces demonstrated by AFM experiments allowed us to consider that the stratification of the thin epoxy–amine films in two layers[23] with different stoichiometries, different crosslinking densities, and various mobilities[24] took place, whatever the whole amine–epoxy ratio before curing, that is, with an initial amine–epoxide ratio ranging from a large excess of amines groups ($r = 1.4$) to a stoichiometric amine–epoxy ratio.[25]

Upper Layer Characterization for the Epoxy–Amine Films about 200 nm Thick. ***Amine enrichment at the air–polymer interface.*** To confirm the enrichment of amines on the surface of the nanostructured thermosets, XPS was used to examine the surface elemental compositions. Shown representatively in Figure 6 are the XPS spectra of the control epoxy–amine bulk sample and the nanostructured thin films in excess amine.

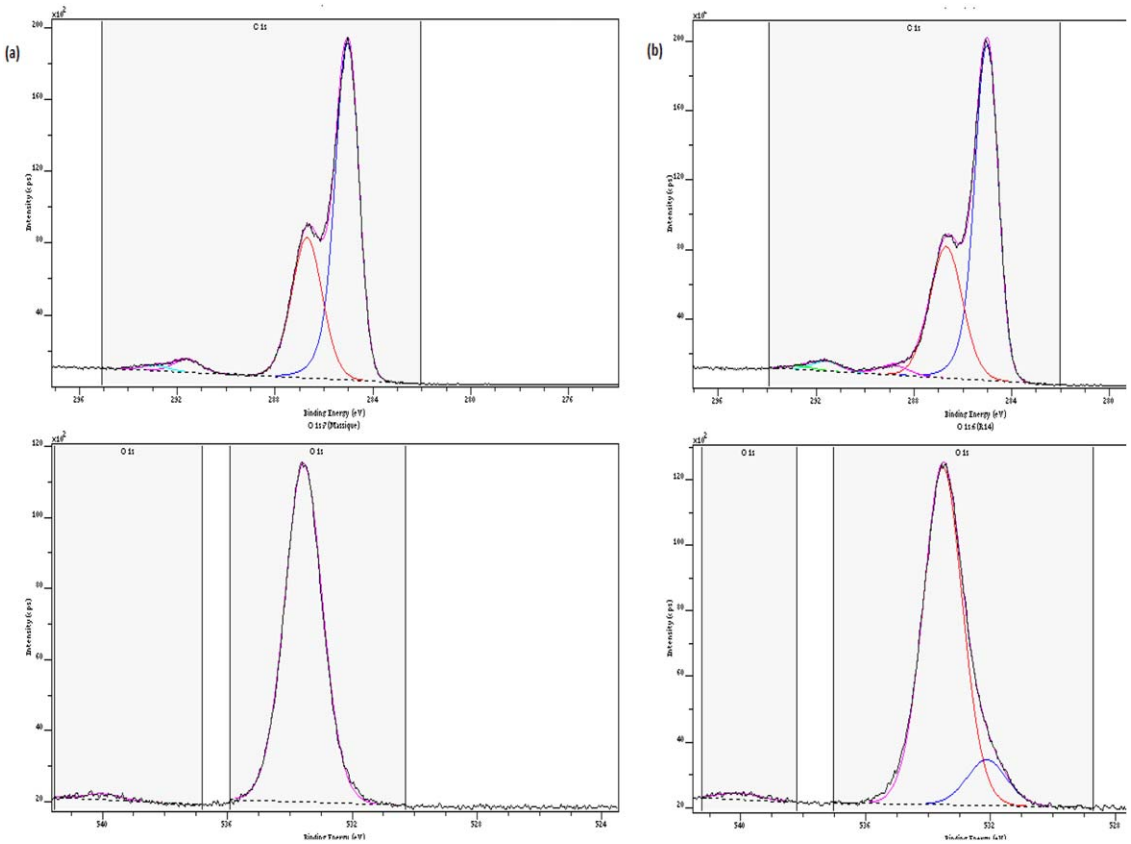

Figure 6. C1s (top) and (O1s) peaks (bottom) in the XPS spectrum: (a) bulk sample at stoichiometric epoxy–amine ratio and (b) thin epoxy–amine of 200 nm for amine-rich films ($r = 1.4$). [Color figure can be viewed in the online issue, which is available at wileyonlinelibrary.com.]

The C1s peak was observed at about 285 eV; this was responsible for the contribution of several kinds of carbon atoms from the epoxy–amine thermosets. The O1s peak was at approximately 533.6 eV. It should be pointed out that the signal of N1s was weaker, and the peak was at 400 eV. The Si atoms from the substrate contributed less than 0.1%, with the Si 2p signals at 105 eV corresponding to a weak contamination of Si^{2+} on the sample surface. The relative concentrations of C, O, N, and Si on the surfaces of the thermoset films, calculated from the corresponding photoelectron peak areas, are listed in Table I. We observed that the carbon and oxygen were dominant on the detected surfaces of all of the nanostructured thermosets and the bulk sample, and a small amount of nitrogen from the DDM moiety was also detected. We noticed that the N/C atomic ratio on the surface of the nanostructured thin thermoset films was significantly higher than the bulk sample value at the stoichiometric ratio. Moreover, the surface contents of N increased with increasing amine in the nanostructured thermosets. For instance, the N/C ratio at the thin film surface was approximatively 4, whereas the expected value should have been 5.2 for an amine–epoxy ratio of 2. Indeed, the XPS results show O═C─O and NH_3^+ on the thin films; this was ascribed to bicarbonate ammonium salt[35,37] induced by atmospheric CO_2 in the presence of a great excess amine, which was not observed for the epoxy–amine bulk sample. This additional amount of adsorbed atmospheric CO_2 increased the C1s amount, and thus reduced the N/C ratio.

This observation suggested that an enrichment of an N-containing moiety existed on the surfaces of the nanostructured thermosets. This result is important for understanding the existence of the vertical structuration layer in the thin thermoset films and for quantitatively characterizing the upper layer composition.

Table I. Elementary Atomic Surface Composition and N/C Atomic Ratio of the Bulk and Thin-Film Samples (Film Thickness ≈ 200 nm) After Curing According to Stage 1

Sample	C (atom %)	N (atom %)	O (atom %)	Si (atom %)	N/C × 100
Bulk ($r = 1$)	84.9	2.8	12.2	< 0.1	3.3
Thin films ($r = 1.13$)	81.7	3.2	15	< 0.1	3.9
Thin films ($r = 1.4$)	81.9	3.4	14.6	< 0.1	4.2

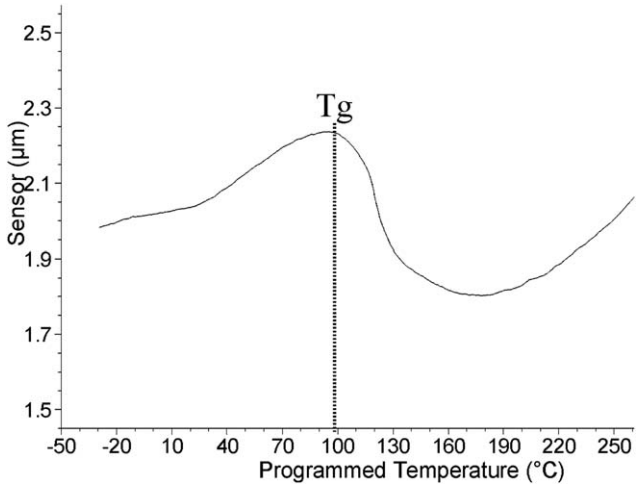

Figure 7. Sensor height position response versus temperature for the bulk epoxy–amine resin ($r = 2$) cured according to stage 1.

Glass-transition properties and stoichiometry in the upper layer. As demonstrated previously[24] and confirmed by the quantitative XPS results, for the amine surface enrichment in the stratified thin film, the lower T_g was ascribed to the upper layer, whereas the higher T_g was ascribed to the film sublayer.

The T_g of the upper layer was close to 95°C (±5°C) for the amine-rich films ($r = 1.4$, Figure 4) and 98°C (±5°C) for the quasi-stoichiometric films ($r = 1.13$).[24,25] We have previously shown that the crosslinking and mobility at the air–network interface were neither affected by the substrate surface nor modified by postcuring.[24,25] Once again, the postcuring of these vertically stratified off-stoichiometric samples did not modify the mobility at the air–network interface. Therefore, we assumed that no more unreacted epoxide functions were present in the upper layer after curing. Moreover, Tillman *et al.*[38] demonstrated that the T_g measured by microthermal analysis in L-TA mode was very sensitive to the crosslinking density. With this property and this technique, different bulk samples in excess amine at the same amine conversion rate and without any more unreacted epoxide groups were used to determine the relationships, with all things being equal between the T_g and the initial stoichiometry. Bulk samples with an amine–epoxy ratio equal to 2 (Figure 7) had a T_g of 98 ± 5°C. We, thus, suggest that the initial amine–epoxide ratio in the upper layer was close to 2 for the amine-rich films ($r = 1.4$) and quasi-stoichiometric films ($r = 1.13$) according to the L-TA measurements. So this value was used to estimate the upper layer stoichiometry.

Thickness of the upper layer. The thickness of the upper layer was calculated from microthermal analyzer measurements as the step height at half-height between the extrapolated tangents according to a procedure described in detail elsewhere.[39] Thus, the upper layer thickness was estimated to be roughly 30 nm for both the amine-rich films and quasi-stoichiometric films.

Table II. Conversion of the Epoxide and Primary Amine Groups in the Sublayer of the Amine-Rich Films ($r_{sublayer} \approx 1.3$ and Film Thickness ≈ 200 nm) and in the Bulk Resin ($r = 1.3$) after Curing According to Stage 1

Sample	Conversion of epoxide groups (%)	Conversion of primary amine groups (%)
Sublayer of the amine-rich film	65	50
Bulk epoxy–amine resin	67	53

As far as we know, this is the first report in the literature showing that the unexpected property of constant upper layer features (stoichiometry, upper layer thickness) was able to be maintained whatever the amine excess. This result is used to finely tune stratification and compositions of each layers.

Sublayer Characterization for Epoxy–Amine Films About 200-nm Thick. Because we know the stoichiometry and the thickness of the upper layer, we deduced the sublayer thickness. With mass balance in the sublayer of various films, we quantified amine–epoxy ratio in this layer before curing,[25] as summarized in Table II. As expected, the amine-rich film sublayer exhibited an excess amine. Therefore, we did not anticipate etherification in the amine-rich film. The T_g of the sublayer was close to 127°C (±5°C) for the amine-rich films ($r = 1.4$) and 142°C (±6°C) for the quasi-stoichiometric films ($r = 1.13$).[24,25] Thus, the highest T_g was obtained for the quasi-stoichiometric films ($r = 1.13$), and T_g decreased for thee off-stoichiometry.[40]

No etherification in the sublayer of amine-rich films. The L-TA measurements made on the bulk DGEBA–DDM resin, prepared with an amine–epoxide ratio of 1.3, and cured according to the same heating schedule (stage 1) used for the thin films showed only one glass-transition at a temperature of 129°C (±8°C; Figure 8).

Moreover, the conversion of the epoxy and primary amine groups in the sublayer of the thin films and in the bulk DGEBA–DDM resin ($r = 1.3$ bulk sample) after curing is reported in Table IV. The FT–IRRAS spectra (Figure 9) also confirmed that side reactions, such as etherification reactions, were negligible in the amine-rich samples (no band at 1120 cm^{-1}).

Thus, the stoichiometry, the conversion of the epoxy and primary amine groups, and the T_g values of the sublayer of the

Table III. Thickness and T_g Values of the Upper Layer According to the Stoichiometry of 200-nm Thin Films After Curing According to Stage 1

Film stoichiometry (r = [Amine]/[Epoxide])	Upper layer stoichiometry (r' = [Amine]/[Epoxide])	Upper layer thickness (nm)	T_g of the upper layer (°C)
1.13	2	30 ± 3 nm	98 ± 5°C
1.4	2	28 ± 3 nm	95 ± 5°C

Table IV. Examples of the Conversion of the Epoxide and Primary Amine Groups in the Sublayers of the Amine-Rich Films (Film Thicknesses = 120–290 nm) after Curing According to Stage 1

Film thickness (nm)	Conversion of epoxide groups (%)	Conversion of primary amine groups (%)
290	64	52
200	65	50
120	61	49

amine-rich films were similar to those of the bulk sample prepared with an amine–epoxide ratio of 1.3 and cured according to the same heating schedule (stage 1). As observed for quasi-stoichiometric films (thickness ≈ 200 nm),[25] the T_g of the amine-rich films did not seem to be affected by a network confinement effect because neither deviation on the T_g nor a conversion rate between the thin layer and the bulk sample were observed. Moreover, although several interface effects could occur (covalent bonds between the silicon substrate and the polymeric network, glassy layer at the substrate interface, etc.), they did not seem to strongly modify the average T_g of the sublayer versus the bulk sample one for thicknesses above 160 nm.[25,34] The network crosslinking density seemed to be the key parameter in defining the glass transition of the 200 nm thick DGEBA–DDM films.

We also noted that a large excess of amine caused a significant shift in the sublayer T_g. Indeed, the sublayer T_g decreased by 15°C in the amine-rich films ($r_{\text{sublayer before curing}} \approx 1.3$) compared to that in the quasi-stoichiometric films ($r_{\text{sublayer before curing}} \approx 1$). In the case of the epoxy–amine bulk samples, Muruyama and Bell[41] indicated that excess amine increased the molecular weight between crosslinks and, thus, decreased T_g. This phenomenon also occurs in polymer films and, thus, explains the decrease in the sublayer T_g observed for the amine-rich films.

These results suggest that during the curing of the excess-amine films, no secondary reactions occurred to induce the same step of reactions as it could be showed in the equivalent stoichiometry or off-stoichiometry bulk sample. The absence of additional topological constraints in the network did not induce a segregation increase of the amine component at the surface.

Therefore, the epoxy–amine segregation in amine-rich films was mainly controlled by the differences in the surface tensions of the components and the evaporation rate of the solvent during spin coating.

Effect of postcuring on the network structure. Polymer films about 200 nm thick were postcured 2 h at 180°C (stage 2) to complete the crosslinking reactions in the sublayer. The results of L-TA measurements made after postcuring again showed the presence of two T_g's. In the case of amine-rich films ($r = 1.4$), no etherification was observed.

The lower T_g, which remained roughly constant after this additional cure, was ascribed to the upper layer, with an initial amine–epoxy ratio close to 2 for amine-rich films. In the upper layer, having a rich composition of amine, the off-stoichiometry was so important that it prevented any postcuring reaction between the amine and epoxy at 180°C. However, its thickness was reduced from 30 to 17 nm for the amine-rich films. So, we assumed that the epoxies of the sublayer and a fraction of the excess amine from the former upper layer (observed after stage 1) reacted during postcuring. Therefore, the upper layer could be divided fictively into two layers (Scheme 1). The thickness of layer 1 was 17 nm. This layer was composed of unreacted amines without any more free epoxy before postcuring, whereas the amine–epoxy ratio still remained close to 2 after postcuring. Layer 2 was 13 nm thick and provided excess amine to the sublayer (layer 3 in Scheme 1) during postcuring. The conservation of matter in the whole film allowed us to estimate the amine–epoxy ratio (r') before postcuring at 180°C in the new fictive sublayer composed of layer 2 (a fraction of the upper layer that was 13 nm thick) and layer 3 (initially called the sublayer after stage 1 curing).

Thus, these layers, which underwent postcuring reactions, presented a large excess of amines ($r' \sim 2$) in the case of amine-rich films. After postcuring, the primary amine–epoxy

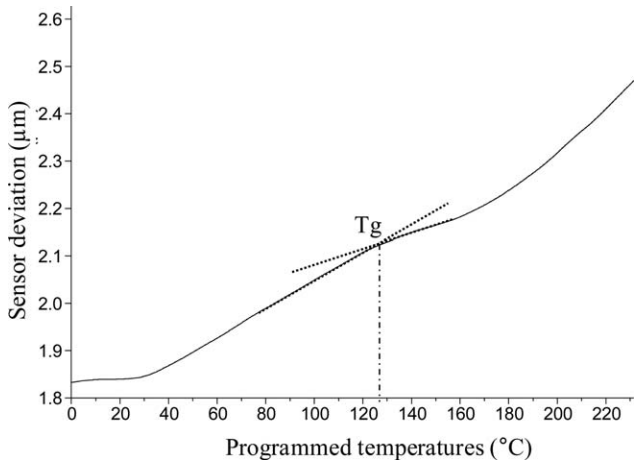

Figure 8. Sensor height position response versus temperature for the bulk epoxy–amine resin ($r = 1.3$) cured according to stage 1.

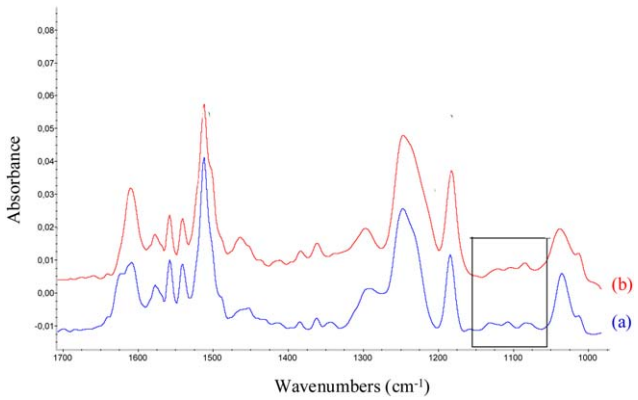

Figure 9. FT–IRRAS spectra in the 1700–975-cm^{-1} region for an amine-rich film ($r = 1.4$) cured on an oxidized wafer (film thickness ≈ 200 nm): (a) before curing and (b) after curing (stage 1). [Color figure can be viewed in the online issue, which is available at wileyonlinelibrary.com.]

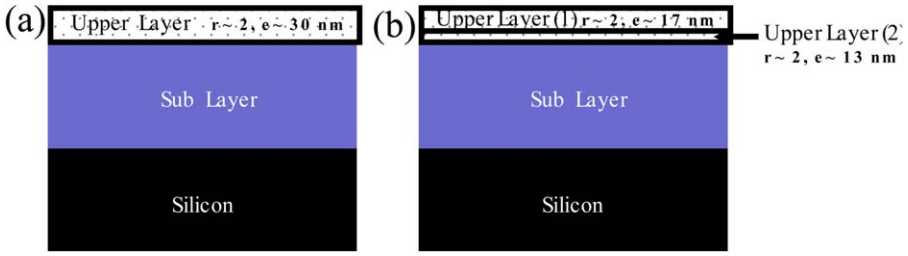

Scheme 1. Stratified layer of an epoxy-rich film with (a) an upper layer of 30 nm and an initial amine–epoxide ratio (r) of about 2 and (b) an upper layer fictively divided into two layers of (1) 17 and (2) 13 nm at the same r value of about 2 before postcuring at 180°. (1b) The upper layer amines and (2b) the sublayer amines and epoxides underwent postcuring. [Color figure can be viewed in the online issue, which is available at wileyonlinelibrary.com.]

conversions in the sublayers (layers 2 and 3) of the amine-rich films were 75 and 100%, respectively.

The higher T_g (i.e., the T_g of the sublayer) thus increased from 127°C to only 147°C for the amine-rich films ($r = 1.4$). Postcuring resulted in an increase in the crosslinking density because of the completion of network formation at 180°C, and this agreed with the T_g increase of the new sublayer (Layer 2 + Layer 3).

Unlike quasi-stoichiometric films,[25] etherification reactions did not occur in the sublayers of the postcured amine-rich films because of the large excess of amines in the sublayers before curing and after stage 1.

The network structure and macromolecular mobility in the sublayers of these postcured amine-rich films were equivalent to those of the postcured bulk sample.[42] These results confirm that the sublayers of the amine-rich films did not seem to be affected by either a network confinement effect or specific interactions of the network with the surface and that the network crosslinking density seemed to be a key parameter in defining the T_g values of the thin DGEBA–DDM films.

In summary, we have shown that the use of vertically nanostructured thin epoxy–amine films afforded us the ability to easily modulate the amine–epoxide ratio in a wide range in the sublayer thanks to the initial amine–epoxy off-stoichiometric mixture. More interestingly, we confirmed that not only could etherification occur at a low curing temperature in excess epoxy and be stopped at high curing temperature when the epoxide groups were no longer in excess after the first curing stage[25] but also that the primary amine conversion related to the epoxy–amine ratio remained constant in the sublayer according to the curing schedule.

Thus, controlling the film thickness, initial epoxy–amine ratio, and cure schedule allowed us to controlled etherification or the lack of etherification versus the epoxy–amine reaction rates at the inorganic interface. Moreover, we easily obtained a controlled network structure from low to very high epoxide or amine conversion through the preparation of different thin films; this was a very difficult task experimentally and very time-consuming in the bulk system. The sensitivity of the thermomechanical properties to the conversion degree underscores the importance of taking into account the degree of curing in the analysis and interpretation of experimental data or theoretical predictions as well as in the design of processing conditions, especially for imbalanced stoichiometric formulations at the interface.

No Evidence of Confinement Effects in the Thin Films

Recently, the effect of the thickness on the thermomechanical response of freestanding thermoset ultrathin films was addressed from molecular dynamics.[28] The depression of ultrathin film properties, Young's modulus, and T_g were assumed to be thickness-dependent below 90 nm. Furthermore, in thermoset polymers, there is also another contributing factor to T_g depression in ultrathin thermoset films: changes in the conversion degree, as describe previously.

To evince that properties variations such as T_g were mainly due to the rate of controlled primary epoxy–amine reactions, all things being equal, we prepared cured thin films with various thicknesses. So, epoxy–amine mixtures of different concentrations in toluene were spin-cast onto oxidized silicon substrates. The amine–epoxy ratios in solution were equal to 1.13 and 1.4. The samples were cured at atmospheric pressure according to stage 1. The concentration of the epoxy solution ranged from 25 to 80 g/L to obtain homogeneous thin films with thicknesses from 90 to 300 nm.

The stratification of thin epoxy–diamine films in two layers with different stoichiometries and different crosslinking

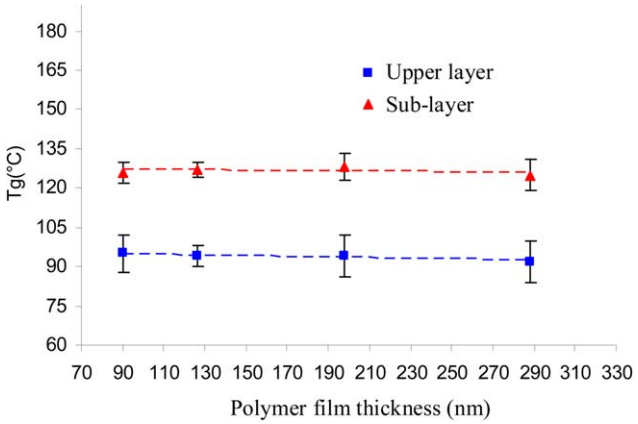

Figure 10. T_g evolution as a function of the film thickness for the two layers of amine-rich films ($r = 1.4$) after curing (stage 1). [Color figure can be viewed in the online issue, which is available at wileyonlinelibrary.com.]

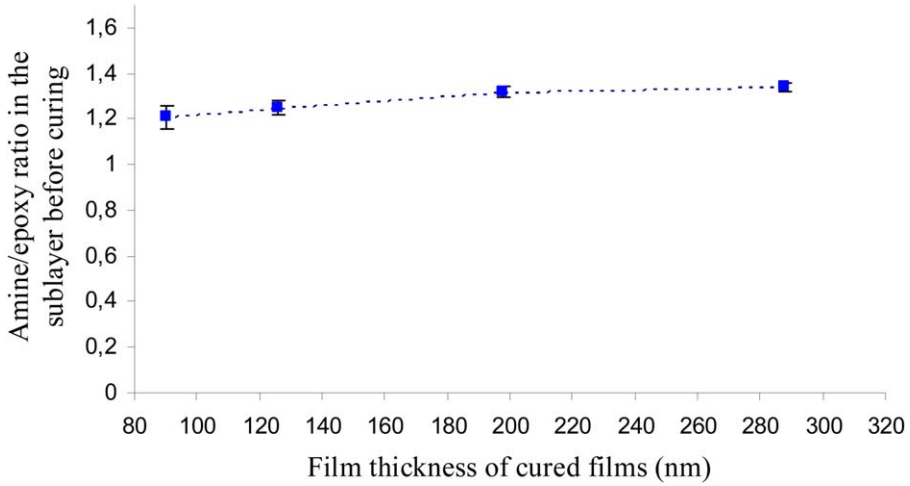

Figure 11. Amine–epoxy ratio as a function of the film thickness in the sublayer of amine-rich films before curing. [Color figure can be viewed in the online issue, which is available at wileyonlinelibrary.com.]

densities took place for the different analyzed films. The T_g evolutions of the two layers after curing as a function of the epoxy–amine film thickness are shown in Figure 10 for the amine-rich films.

Upper Layer Properties. In the case of amine-rich and quasi-stoichiometric films, the T_g of the layer at the air–network interface remained close to 95–100°C (Figure 10)[32] for the amine-rich films. Thus, we noted that the T_g of the upper layer was not affected by the film thickness, whatever the initial composition. We noted that for the different initial stoichiometries used, the upper layer thickness, calculated from microthermal analyzer measurements, remained roughly constant, whatever the film thickness, according to the stoichiometry.

Thus, we concluded that whatever the whole amine–epoxide ratio in films before curing, the upper layer stoichiometry and thickness were not affected by the total film thickness. These results seem to indicate that during the synthesis of epoxy–amine films, the amount of amine functions migrating to the air–film interface did not depend on the film thickness.

Sublayer Properties. Indeed, the T_g of the sublayer remained close to 127°C (± 5°C) for the amine-rich films ($r = 1.4$), whatever the film thickness (Figure 10). Unlike quasi-stoichiometric films,[25] the T_g of the sublayer in the amine-rich was not affected by the film thickness.

In the case of amine-rich films with thicknesses in the range 90–300 nm, the initial amine–epoxy ratio in the sublayer varied between 1.2 and 1.3 (Figure 11). Indeed, whatever the film thickness, the sublayer remained with an excess of amine groups before curing, despite the preferential segregation of the cross-linker at the air–surface. The FT–IRRAS spectra (Figure 12) also confirmed that side reactions (etherification reactions) were negligible in the amine-rich films, whatever their thicknesses (there was no band at 1120 cm^{-1}). The conversion of the epoxide and primary amine groups in the sublayer of the amine-rich films after curing according to the stage 1 is reported in Table IV. We thus noted that the conversion of the epoxide and primary amine groups was independent of the film thickness in the range 90–300 nm.

To summarize, the stoichiometry, crosslinking reactions, and conversion of the epoxy and primary amine groups in the sublayer of the amine-rich films were similar, whatever the film thickness. Similar thermoset networks were thus created in the sublayer of the amine-rich films for the different film thicknesses analyzed, and the sublayer T_g was not affected by the film thickness. For films between 90 and 300 nm, we concluded from these results that no additional confinement effect from the air–surface interface resulting in the reduction of the T_g could be ascribed to the T_g of the upper layer measured for the stratified thin films. The T_g of the upper layer was mainly ascribed to the enrichment of the amine at the film's air–surface interface.

Although several equations to describe T_g versus conversion data have been used in the literature,[43–45] this can still be

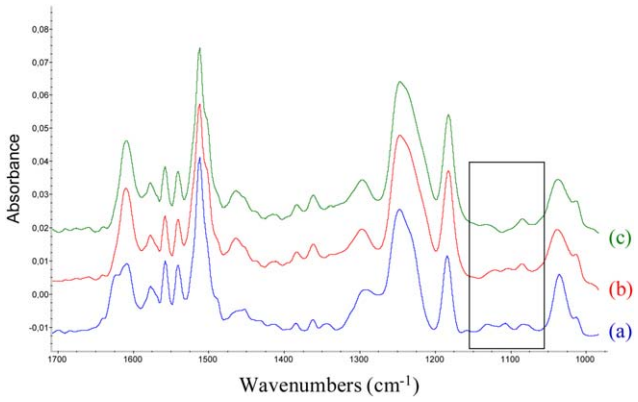

Figure 12. FT–IRRAS spectra in the 1700–975-cm^{-1} region for an amine-rich film ($r = 1.4$) cured on an oxidized wafer: (a) before curing and (b) after curing (stage 1) for a film thickness of about 200 nm and (c) after curing (stage 1) for a film thickness of about 120 nm. [Color figure can be viewed in the online issue, which is available at wileyonlinelibrary.com.]

considered an unsolved problem, particularly for systems with imbalanced stoichiometry[22] usually used in coating and composites technologies. Therefore, it should be a facile route to access missing experimental data to improve these equations according to the curing schedule, especially for limited conversion rates. However, to completely fulfill these data, further studies should be done on potential different constraint levels between thin films and bulk samples introduced by crosslinks in high crosslinking networks. This must be investigated further.

CONCLUSIONS

In this study, we demonstrated that the use of thin epoxy–amine films is a powerful tool for overcoming challenging experimental difficulties in controlling the degree of curing and the quantitative monitoring of epoxy–amine off-stoichiometry at the silica interface. In fact, DGEBA–DDM supported thin films can be easily nanostructured into two layers, in which the upper one has controlled specifications and are only dependent on the sample preparation, and on the resulting amine–epoxy ratio in this layer over a wide range of amine–epoxy compositions. The intensity of DDM segregation at the air–surface, which is at the origin of this layer stratification, seemed to be controlled in amine composition excess by the differences in the surface tensions of the components and the solvent evaporation rate during spin-coating. Thus, these parameters are set, and the T_g of this surface layer is constant, regardless of the film thickness between 100 and 300 nm, the curing schedule, or the silica surface chemistry.[24]

This unusual property is used to vary in a controlled manner the sublayer composition and promote chemically controlled reactions, including or avoiding etherification compared to epoxy–amine crosslinking. The network structure is well tuned still, and the T_g can be finely measured by microthermal analysis, which is a convenient technique for obtaining T_g on a local scale in relation to the network density.

Our results show that under excess amine, the epoxy–amine reactivity and the resulting network were the same as the bulk ones.

Interestingly, the primary amine conversion degree related to the epoxy–amine ratio was also constant in the sublayer, whatever the imbalance stoichiometry in excess amine. Hence, different network structures were finely tuned, depending on the curing schedule, deviation from the stoichiometry, and film thickness, to modulate the stoichiometry in the sublayer. The data thus obtained should be used by simulations to improve the predicted structural network properties of coatings at interfaces with regard to usual off-stoichiometric formulations in thermoset resins. We can speculate that once the connections between chemistry and atomic interactions and the macroscopic world are established and validated, predictive computational tools will facilitate the design of new thermoset thin films; this will reduce the need for time-consuming and expensive experiments. Our methodology with thin films, which is very versatile, less expensive, and completed by local elastic modulus analysis, presented in a forthcoming article, should be used to validate these connections in thermoset thin films.

ACKNOWLEDGMENTS

This work was supported by a doctoral fellowship to Sandra Onard from the French Ministry of Research.

REFERENCES

1. Jones, F. R. *Key Eng. Mater.* **1996**, *41*, 116.
2. DiBenedetto, A. T. *Mater. Sci. Eng. A* **2001**, *74*, 302.
3. Knorr, D. B., Jr.; Yu, I. H.; Richardson, A. D.; Hindenlang, M. D.; McAninch, I. A.; La Scala, J. J.; Lenhart, J. L. *Polymer* **2012**, *53*, 5917.
4. Sahagun, C.; Morgan, S. *ACS Appl. Mater. Interfaces* **2012**, *4*, 564.
5. Feng, J. F.; Berger, K.; Douglas, E. P. *J. Mater. Sci.* **2004**, *39*, 3414.
6. Choi, S.; Douglas, E. P. *ACS Appl. Mater. Interfaces* **2010**, *2*, 934.
7. Yung, K.; Zhu, B.; Yue, T.; Cie, C. *J. Appl. Polym. Sci.* **2010**, *116*, 518.
8. Ellis, B.; Found, M.; Bell, J. *J. Appl. Polym. Sci.* **2001**, *82*, 1265.
9. Lesser, A. J.; Crawford, E. *J. Appl. Polym. Sci.* **1997**, *66*, 387.
10. Lesser, A. J.; Crawford, E. *J. Polym. Sci. Part B: Polym. Phys.* **1998**, *36*, 1371.
11. Sue, H.-J.; Puckett, P. M.; Bertram, J. L.; Walker, L. L.; Garcia-Meitin, E. I. *J. Polym. Sci. Part B: Polym. Phys.* **1999**, *37*, 2137.
12. Simpson, J. O.; Bidstrup, S. A. *J. Polym. Sci. Part B: Polym. Phys.* **1995**, *33*, 55.
13. Knorr, D. B., Jr.; Jaye, C.; Fischer, D. A.; Shoch, A. B.; Lenhart, J. L. *Langmuir* **2012**, *28*, 15294.
14. Yang, L.; Hristov, H. A.; Yee, A. F.; Gidley, D. W.; Bauchiere, D.; Halary, J.-L.; Monnerie, L. *Polymer* **1995**, *36*, 3997.
15. Soles, C. L.; Chang, F. T.; Bolan, B. A.; Hristov, H. A.; Gidley, D. W.; Yee, A. F. *J. Polym. Sci. Part B: Polym. Phys.* **1998**, *36*, 3035.
16. Soles, C. L.; Yee, A. F. *J. Polym. Sci. Part B: Polym. Phys.* **2000**, *38*, 792.
17. Soles, C. L.; Chang, F. T.; Gidley, D. W.; Yee, A. F. *J. Polym. Sci. Part B: Polym. Phys.* **2000**, *38*, 776.
18. Bidstrup, S. A.; Simpson, J. O. *J. Polym. Sci. Part B: Polym. Phys.* **1995**, *33*, 43.
19. Drzal, L. T. *Adv. Polym. Sci.* **1986**, *75*, 1.
20. Palmese, G. R.; McCullough, R. L. *J. Appl. Polym. Sci.* **1992**, *46*, 1863.
21. Gupta, V. B.; Drzal, L. T.; Lee, C. Y.-C; Rich, M. *J. Polym. Eng. Sci.* **1985**, *25*, 812.
22. Meyer, F.; Sanz, G.; Eceiza, A.; Mondragon, I.; Mijović, J. *Polymer* **1995**, *36*, 1407.
23. Yim, H.; Kent, M.; Ivkov, R.; Satija, S.; Majewski, J. *Macromolecules* **1999**, *32*, 7932.
24. Carriere, P.; Onard, S.; Mallarino, S. *Surf. Interface Anal.* **2009**, *41*, 858.
25. Onard, S.; Martin, I.; Chailan, J. F.; Crespy, A.; Carriere, P. *Macromolecules* **2011**, *44*, 3485.

26. Wang, X.; Zhou, W. *Macromolecules* **2002**, *35*, 6747.
27. Price, D. M.; Reading, M.; Hammiche, A.; Pollock, H. M.; Branch, M. G. *Thermochim. Acta* **1999**, *332*, 143.
28. Li, C.; Strachan, A. *Macromolecules* **2011**, *44*, 9448.
29. Lenhart, J. L.; Wu, W. *Macromolecules* **2002**, *35*, 5145.
30. Price, D. M.; Reading, M.; Hammiche, A.; Pollock, H. M.; Branch, M. G. *Eur. Ed.* **1998**, *53*, 21.
31. Hong-Bo, L.; Nagaiyanallur, V.; Bauert, T. E; Marcus Textor, M.; Xiao, S.-J. *J. Phys. Chem. A* **2008**, *112*, 12372.
32. Christopher, J. G.; Glenn, R. H.; Taylor, J. W. *Anal. Chem.* **1994**, *66*, 1015.
33. Gupta, V. B.; Drzal, L. T.; Adams, W. W.; Omlor, R. *J. Mater. Sci.* **1985**, *20*, 3439.
34. Pascault, J. P.; Duchet, J. *Polym. Sci. Part B: Polym. Phys.* **2003**, *41*, 2422.
35. Giraud, M.; Nguyen, T.; Gu, X.; VanLandingham, M. R. *Annu. Meet. Adhes. Soc.* **2001**, *24*, 260.
36. Vanlandingham, M. R.; Eduljee, R. F.; Gillespie, J. W., Jr; . *J. Appl. Polym. Sci.* **1999**, *71*, 699.
37. Bell, J. P.; Reffner, J. A.; Petrie, R. *J. Appl. Polym. Sci.* **1977**, *21*, 1095.
38. Tillman, M. S.; Takatoya, T.; Hayes, B. S.; Seferis, J. C. *J. Therm. Anal. Calorim.* **2000**, *62*, 599.
39. Van Assche, G.; Ghanem, A.; Lhost, O.; Van Mele, B. *Polymer* **2005**, *46*, 7132.
40. Matejka, L. *Macromolecules* **2000**, *33*, 3611.
41. Murayama, T.; Bell, J. P. *J. Polym. Sci. Part A-2: Polym. Phys.* **1970**, *8*, 437.
42. Dusek, K. *Polym. Bull.* **1985**, *13*, 321.
43. DiBenedetto, A. T. *J. Polym. Sci. Part B: Polym. Phys.* **1987**, *25*, 1949.
44. Pascault, J. P.; Williams, R. J. J. *J. Polym. Sci. Part B: Polym. Phys.* **1990**, *28*, 85.
45. Hale, H.; Macosko, C. W. *Macromolecules* **1991**, *24*, 2610.